Structural Features of Membrane Fusion between Influenza Virus and Liposome as Revealed by Quick-Freezing Electron Microscopy

Toku Kanaseki,* Kazunori Kawasaki,‡ Masayuki Murata,§ Yoko Ikeuchi,* and Shun-ichi Ohnishi§

*Department of Cell Biology, Tokyo Metropolitan Institute for Neuroscience, Tokyo 183; ‡Cellular Biophysics Laboratory, National Institute of Bioscience and Human Technology, Tsukuba 305; and §Department of Biophysics, Faculty of Science, Kyoto University, Kyoto 606, Japan

Abstract. The structure of membrane fusion intermediates between the A/PR/8(H1N1) strain of influenza virus and a liposome composed of egg phosphatidylcholine, cholesterol, and glycophorin was studied using quick-freezing electron microscopy. Fusion by viral hemagglutinin protein was induced at pH 5.0 and 23°C. After a 19-s incubation under these conditions, small protrusions with a diameter of 10–20 nm were found on the fractured convex faces of the liposomal membranes, and small pits complementary to the protrusions were found on the concave faces. The protrusions and pits corresponded to fractured parts of outward bendings of the lipid bilayer or "microprotrusions of the lipid bilayer." At the loci of the protrusions and pits, liposomal membranes had local contacts with viral membranes. In many cases both the protrusions and the pits were aligned in regular polygonal arrangements, which were thought to reflect the array of hemagglutinin spikes on the viral surface. These structures were induced only when the medium was acidic with the virus present. Based on these observations, it was concluded that the microprotrusions of the lipid bilayer are induced by hemagglutinin protein. Furthermore, morphological evidence for the formation of the "initial fusion pore" at the microprotrusion was obtained. The protrusion on the convex face sometimes had a tiny hole with a diameter of <4 nm in the center. The pits transformed into narrow membrane connections <10 nm in width, bridging viruses and liposomes. The structures of the fusion pore and fusion neck with larger sizes were also observed, indicating growth of the protrusions and pits to distinct fusion sites. We propose that the microprotrusion of the lipid bilayer is a fusion intermediate induced by hemagglutinin protein, and suggest that the extraordinarily high curvature of this membrane structure is a clue to the onset of fusion. The possible architecture of the fusion intermediate is discussed with regard to the localization of intramembrane particles at the microprotrusion.

Viral membrane fusion is widely accepted as a paradigm for biological membrane fusion mechanisms (Monck and Fernandez, 1992; White, 1992). In particular, hemagglutinin (HA)[1] of influenza virus is the best characterized among fusogenic membrane glycoproteins (for reviews see Hughson, 1995; Carr and Kim, 1994; Brunner and Tsurudome, 1993; Stegmann and Helenius, 1993; Clague et al., 1993; Wilschut and Bron, 1993; Bentz et al., 1993; Wiley and Skehel, 1987). HA possesses fusion activity only at acidic pH (<pH 5.5), which is used for control of viral fusion with endosomal membranes in the course of viral infection of host cells. The pH-dependent conformational changes in HA and insertion of the "fusion peptide" of the protein into target membranes are considered to be the trigger that induces fusion.

HA is synthesized as a trimeric form of monomers with an approximate molecular weight of 84,000. The precursory form of HA is converted to a fusion-active form by posttranslational cleavage; each HA monomer is cleaved into two polypeptide chains, HA1 and HA2 (Klenk et al., 1975; Lazarowitz and Choppin, 1975; Maeda et al., 1981; for review, see Air and Laver, 1986; White, 1990). According to the three-dimensional structure of HA determined by x-ray crystallography (Wilson et al., 1981), the trimeric HA spike has a height of 135 Å from the surface of the viral membrane. The receptor binding site of HA1 is on the

Address all correspondence to Toku Kanaseki, The Department of Cell Biology, Tokyo Metropolitan Institute for Neuroscience, 2-6 Musashidai, Fuchu City, Tokyo 183, Japan. Tel.: 81-423-25-3881. Fax: 81-423-21-8678.

Shun-ichi Ohnishi's present address is The Department of Materials Chemistry, Faculty of Science and Technology, Ryukoku University Seta Campus, 1-5 Yokoya, Seta Ohe-Cho, Ohtsu, Shiga 520-21 Japan.

1. *Abbreviations used in this paper*: ESR, elecron spin resonance; HA, hemagglutinin; IMP, intramembrane particle; NA, neuroaminidase.

top region of the spike, and the fusion peptide, ~20 amino acid residues at the amino terminal of HA2 (Gething et al., 1978; Gething et al., 1986), is located ~35 Å from the viral membrane, >100 Å apart from the target membrane. In spite of the extensive characterization of this protein, basic questions about the molecular mechanism of HA-mediated membrane fusion, such as how HA causes close apposition of two membranes and the type of fusion intermediate formed by HA, are still unanswered (Hughson et al., 1995; Carr and Kim, 1994).

In this study, we have investigated the structural features of membranes during fusion between influenza virus and liposomes using EM. Since the process of viral fusion with liposomes is completed very rapidly (within 1 min at pH 5.0–5.2 and 37°C; Maeda et al., 1981; White et al., 1982; Stegmann et al., 1985; Stegmann et al., 1990; Kawasaki and Ohnishi, 1992), it is impossible to analyze the structural sequence of fusion events using conventional EM methods. Although numerous biochemical and biophysical studies of virus and membrane fusion activity have been reported (for reviews see Ohnishi, 1988; Stegmann et al., 1989; White, 1990; White, 1992; Stegmann and Helenius, 1993), and several EM studies have been published (Matlin et al., 1981; Yoshimura et al., 1985; Stegmann et al., 1990), there are only a few reports concerning HA-induced fusion studied using quick-freezing replica techniques (Knoll et al., 1988; Burger et al., 1988). To clarify the intermediary steps of membrane fusion, we took advantage of the deep-etch replica technique developed by Heuser (1981).

The following points are discussed. (*a*) Fusion intermediate: previous kinetic studies of HA-induced fusion demonstrated a delay time preceding the onset of fusion and suggested the involvement of prefusion states (Morris et al., 1989; Sarkar et al., 1989; Stegmann et al., 1990; Ludwig et al., 1995). Several models for fusion intermediates have been proposed (Stegmann et al., 1990; Bentz et al., 1990; Guy et al., 1992; Wilschut and Bron, 1993; Bentz et al., 1993; Carr and Kim, 1994). However, no direct morphological evidence for these models has been presented. In this study, we show that HA induces "microprotrusions of the lipid bilayer" in the precursory stage of fusion, and we propose a fusion mechanism via this novel membrane structure as an intermediate.

(*b*) Structural features of the "initial fusion pore": Spruce et al. (1989) studied fusion between HA-expressing cells (HAb-2) and RBC using fluorescence microscopy and patch-clamp electrophysiology. They proposed that the earliest event was the sudden opening of an aqueous pore with a diameter of <4 nm between the two fusing cells (for review see Monck and Fernandez, 1992). Here we demonstrate, by direct EM observations, the formation of the initial fusion pore from the fusion intermediate and its dilation to accomplish the fusion event.

(*c*) Multiple fusion sites on a single viral particle: we often observed that a single viral particle causes multiple fusion intermediates arranged in a polygon on the target liposome membranes. The fusion event seems to proceed simultaneously on each fusion intermediate. We elucidated morphologically the sequence of the "single-point" and "multi-point" fusion events.

(*d*) Structural changes in HA spikes under fusion-competent conditions: several lines of evidence (e.g., Harter et al., 1989; Brunner, 1989) suggest that the fusion peptide is involved in the fusion event. The distance of >100 Å between the fusion peptide and the target membrane at neutral pH must be somehow shortened at acidic pH for the peptide to be inserted into the lipid bilayer. To explain this process, several models assuming drastic conformational changes in HA have been proposed (White and Wilson, 1987; Stegmann et al., 1989, 1990). In this study, however, we did not detect these assumed drastic changes in the spike structure on our quick-frozen replicas; no obvious bending, tilting, or opening of spikes was observed under fusion-competent conditions.

(*e*) Molecular architecture of fusion intermediate: most of the proposed models for HA-induced fusion intermediates have commonly postulated alignment of several HA spikes closely surrounding the fusion site (Stegmann et al., 1990; Bentz et al., 1990; Guy et al., 1992; Bentz, 1993; Wilschut and Bron, 1993). We discuss the molecular architecture of the fusion intermediate by examining the localization of intramembrane particles (IMPs) at the fusion sites.

Materials and Methods

Materials

Influenza virus A/PR/8(H1N1) was grown in embryonated chicken eggs and partially purified as described earlier (Maeda et al., 1975). Virus stock further purified by sucrose density gradient centrifugation was stored at −80°C until use. HA was purified from viral membrane in the form of rosettelike aggregates, as described previously (Kawasaki et al., 1983). Viral protein was assayed by Lowry's method (Lowry et al., 1951) with BSA as a standard. Egg yolk phosphatidylcholine was purified as described by Singleton et al. (1965). The concentration of phospholipid was determined by phosphorus assay (Bartlett, 1959). Cholesterol was purchased from Wako Chemical Co. Ltd. (Osaka, Japan) and recrystallized before use. Glycophorin was purified from human RBC membrane following the procedure of Segrest et al. (1979), and stored at −80°C.

Liposomes containing glycophorin were prepared essentially as described by MacDonald and MacDonald (1975). Aliquots of glycophorin in 10 μl water were added to 2 ml chloroform/methanol (2:1) containing a lipid mixture (4 mg phosphatidylcholine and 1 mg cholesterol) and dried in a test tube. Then 1 ml Pipes buffer (5 mM Pipes-NaOH, 145 mM NaCl, pH adjusted to 7.4) was added with several glass beads, and the tube was gently shaken for 15 min at 37°C. The resulting dispersion was centrifuged for 5 min at 4°C to obtain the pellet, which was suspended in the original volume of Pipes buffer.

To characterize the interaction between the virus and the glycophorin-bearing liposome quantitatively, binding and fusion of spin-labeled influenza virus with the liposomes was assayed essentially as described (Kawasaki and Ohnishi, 1992). Spin-labeled virus (37 μg of total protein) in 50 μl Pipes buffer was mixed with 150 μg liposomes in 200 μl Pipes buffer. The mixture was kept for 10 min at 4°C and then centrifuged at 12,000 *g* for 5 min. The pellet was suspended in 20 μl of 20 mM Na-citrate, 130 mM NaCl, pH 5.0, and transferred to a quartz capillary tube at 4°C. Fusion efficiency (percent) after 5 min at 37°C was estimated from the increase in the electron spin resonance (ESR) peak height. As an assay of viral binding to liposomes, the amount of spin-label in the pellet was estimated from the total intensity of the ESR signal and converted to the amount of viral total protein.

Fig. 1 shows the effect of incorporation of glycophorin into liposomes on viral binding and fusion. The virus bound to and fused even with receptor-free liposomes, although not efficiently, consistent with earlier studies (Maeda et al., 1981, White et al., 1982, Stegmann et al., 1986, Kawasaki and Ohnishi, 1992). Inclusion of glycophorin into liposomes at a receptor/lipid ratio exceeding 0.5% (by weight) increased the fusion efficiency from 17 to ~60%. The enhancement of viral fusion was receptor specific because the fusion efficiency for glycophorin-liposomes treated with neuraminidase was almost the same as that for glycophorin-free liposomes (data not shown). By contrast, enhancement of viral binding by glycopho-

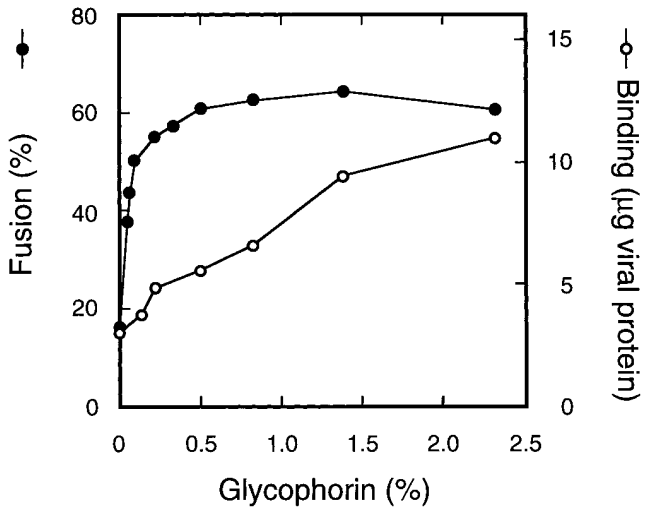

Figure 1. Enhancement of binding (*clear circles*) and fusion (*solid circles*) of spin-labeled influenza virus with liposomes by incorporation of glycophorin into the liposomes (see Materials and Methods). For the binding assay, the amount of virus cosedimented with the liposomes was estimated from the total ESR signal. Because the virus bound even to liposomes without glycophorin, it is clear that the virus caused both receptor-specific binding and nonspecific binding with the glycophorin liposomes. Fusion efficiency was estimated from the increase of the ESR peak height after 5 min at pH 5.0 and 37°C. Fusion was enhanced by a much lower concentration of glycophorin than was the case for binding.

rin was much less marked. Although viral binding was increased twofold by adding 1.0% glycophorin, it was below the saturation level. For the EM experiments described below, we used liposomes with 1% glycophorin at all times. The results shown in Fig. 1 confirm that the virus efficiently fuses with liposomes containing 1% glycophorin. It is also evident that the pellet obtained from the virus and liposome mixture contains both specifically and nonspecifically bound virions.

Samples for Quick-Freezing

(*a*) Influenza virus (total protein 80 μg) in 40 μl Pipes buffer was mixed with 220 μg liposomes in 260 μl Pipes buffer. The mixture was kept for 15 min at 4°C and then centrifuged at 12,000 *g* for 5 min to obtain the pellet.

Membrane fusion was triggered at pH 5.0 and 23°C by mixing 15 μl of the pellet with 3 μl of acidic buffer (80 mM Na-citrate, 70 mM NaCl, pH adjusted to 4.6).

Three mixtures were incubated for 19 s, 30 s, and 2 min, respectively, at 23°C before quick-freezing. As a control at neutral pH , the pellet was suspended in Pipes buffer and incubated for 30 s at 23°C before being processed for quick-freezing.

(*b*) For the experiment using purified HA rosettes and liposomes, 200 μg HA rosettes was mixed in place of the virus using the protocol described in *a* and incubated for 30 s.

(*c*) Viruses incubated for 30 s at pH 5.0 and 23°C were processed by the mica flake technique (Heuser, 1983). As a control, viruses were also processed at neutral pH and 23°C for 30 s.

(*d*) Viruses alone incubated for 30 s at acidic and neutral pH, and liposomes alone incubated for 30 s at acidic pH were also processed for quick-freezing.

EM

The samples were quickly frozen using the technique of Heuser (1981). The frozen materials were fractured and then etched for 2 min in a Balzers BAF 300 (Balzers Union, Balzers, Liechtenstein) with the electron beam gun mounted at 20° relative to the etched surface, to obtain replicas. The replicas were observed with an electron microscope (model JEM 200 CX; JEOL, Akishima, Japan) operating at 200 kV.

Results

Shape of Spikes at Neutral and Acidic pH

Fig. 2 shows the appearance of viruses on replicas at neutral pH. The viruses were ~120 nm in diameter and were homogeneously distributed when observed at low magnification (Fig. 2 *a*). The fracturing split the viral membrane along its hydrophobic interior, resulting in two kinds of fracture face (Fig. 2 *b*), the P-face and the E-face. Etching revealed that the external surface of the viruses was covered with many spikes. The viral membrane is known to have two kinds of spikes, HA and neuraminidase (NA). Although it appears difficult to clearly distinguish the two types on a replica, the spikes which seem to have relatively slender stalks connected to a P-face may be NA spikes (Fig. 2 *b*, *arrows*). The molecular ratio of HA to NA has been reported to be 5:1 (for review see Skehel et al., 1980). Note the size of the IMPs. The particles on the E-face were slightly smaller than those on the P-face.

After the medium containing the viruses had been adjusted to pH 5.0, the samples were incubated for 30 s at 23°C, followed by replication (Fig. 3). Although fusion between viruses and liposomes should already have been under way by this time, the low pH had no detectable influence on the appearance of the HA spikes (Fig. 3, *a* and *d*). No bending, tilting, opening, or lengthening was detected in >90% of spikes on the replicas.

EM observations using negative staining by Ruigrok et al. (1986) demonstrated that HA spikes on viral particles (X-31 strain) and reconstituted vesicles were elongated by 1–2 nm on average after treatment at pH 5 for 10 min. Since the resolution afforded by our EM technique with replication was not as high as 1–2 nm, it was impossible for us to detect this scale of elongation. Ruigrok et al. also indicated that in purified HA rosettes, the spikes are much more elongated—to 21.1 nm on average—by low pH treatment. In addition, in aggregates of bromelain-released hemagglutinin induced by low pH treatment, the spikes were elongated to 17.2 nm on average. However, our observations also did not reveal such extensive elongation of the spikes. This discrepancy might have been due to the difference in the incubation time under low pH conditions; the incubation conducted by Ruigrok et al. was for 10 min, whereas our incubation was for 30 s. Alternatively, the discrepancy might have been due to the EM techniques used; although they negatively stained their samples, we quickly froze the samples without chemical fixation or staining. Our finding that the overall structure of HA spikes does not alter under fusion-competent conditions seems consistent with the cryo-EM observations reported by Booy (1993).

However, it was noteworthy that at low magnification (Fig. 3 *b*), viruses in acidic media showed a tendency to aggregate with each other. Most of the HA spikes were ~14 nm long, whereas spikes at sites of contact between two viruses (Fig. 3 *b*, *arrows*) were apparently shorter than the other spikes. In rare cases, short spikes were also observed on solitary virions (Fig. 3 *c*, *s*), although it was not clear

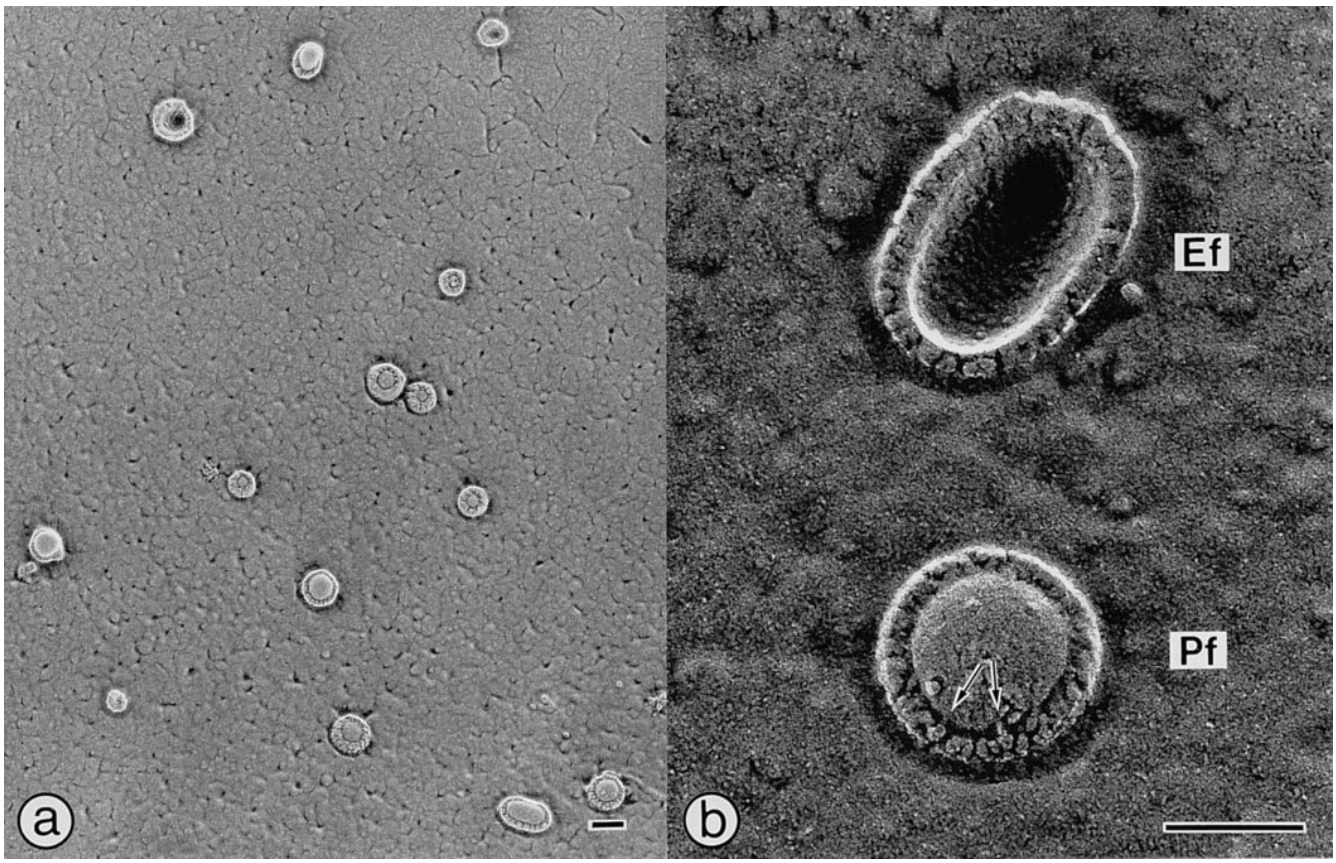

Figure 2. Influenza viruses at pH 7.4 and 23°C. (*a*) Viruses 120 nm in diameter are distributed homogeneously. (*b*) A high magnification electron micrograph of two virions. Compare the size of IMPs on a P-face (*Pf*) to that of IMPs on an E-face (*Ef*). The measured diameter of IMPs on the E-face is ~6 nm. Arrows indicate what could be stalks of NA spikes. Bars, 100 nm.

whether the shortening was due to the acidification process itself or to freeze-fracturing.

Shape of Viruses on Mica Flakes

To obtain a closer view of the virus on replicas, we used the mica flake technique. This involved mixing specimens with an aqueous suspension of tiny flakes of mica, followed by quick-freezing for replication. However, this technique significantly altered the shape of the viral particles incubated in medium at pH 5.0, as compared with those incubated at pH 7.4. As shown in Fig. 4, *b* and *c*, at pH 5.0 and 23°C, viruses were adsorbed on the surface of the mica and appeared to be deformed either by some external force or because of the adsorption itself. Moreover, observation of the fractured E-face suggested that the adsorption was so tight that the viral half membrane was as flat as the mica surface. This distorted shape of the virus particles suggested that they had struck the hard surface of the mica so violently that the spikes in the center were pushed back and everted to form projections on the E-face.

By contrast, on the mica surface at pH 7.4 (Fig. 4 *a*), the viruses appeared to have landed very softly, leaving the overall shape of the virus undisturbed. This could be seen better in side-by-side comparisons; the viruses shown in Fig. 4 *c* were fractured and etched at pH 5.0, whereas those in Fig. 4 *d* were processed identically at pH 7.4. The fractured viruses on the mica after processing at pH 7.4 showed a natural curvature without everted spikes on the E-faces, similar to those fractured in ice (see Figs. 2 and 3).

These results indicate that under the fusion-competent condition (at pH 5.0 and 23°C, for 30 s) the overall structure of the HA spike does not alter, although the nature of the spike is somehow changed so that it interacts strongly with the surface of mica.

Viruses and Liposomes at Neutral pH

As a control for the "fusion experiments" under acidic conditions, influenza virus and liposomes were mixed at pH 7.4, and incubated for 30 s at 23°C. The liposomes were composed of 80% egg phosphatidylcholine, 20% cholesterol, and 1% erythrocyte glycophorin, the viral receptor. Although the liposomes contained the receptor, some of the virions were not attached to the surface of the liposomes, as shown in Fig. 5, *a* and *b.* These free particles may have been nonspecifically bound virions, which were released from liposomes between the centrifugation and quick-freezing steps because of unstable binding (see *Materials and Methods*). However, the other virions were shown to be located on the surface or in the vicinity of the liposomes, and most of these may have corresponded to virions that were bound specifically to the receptor. Even at these binding sites, the fractured convex faces (Fig. 5, *a*

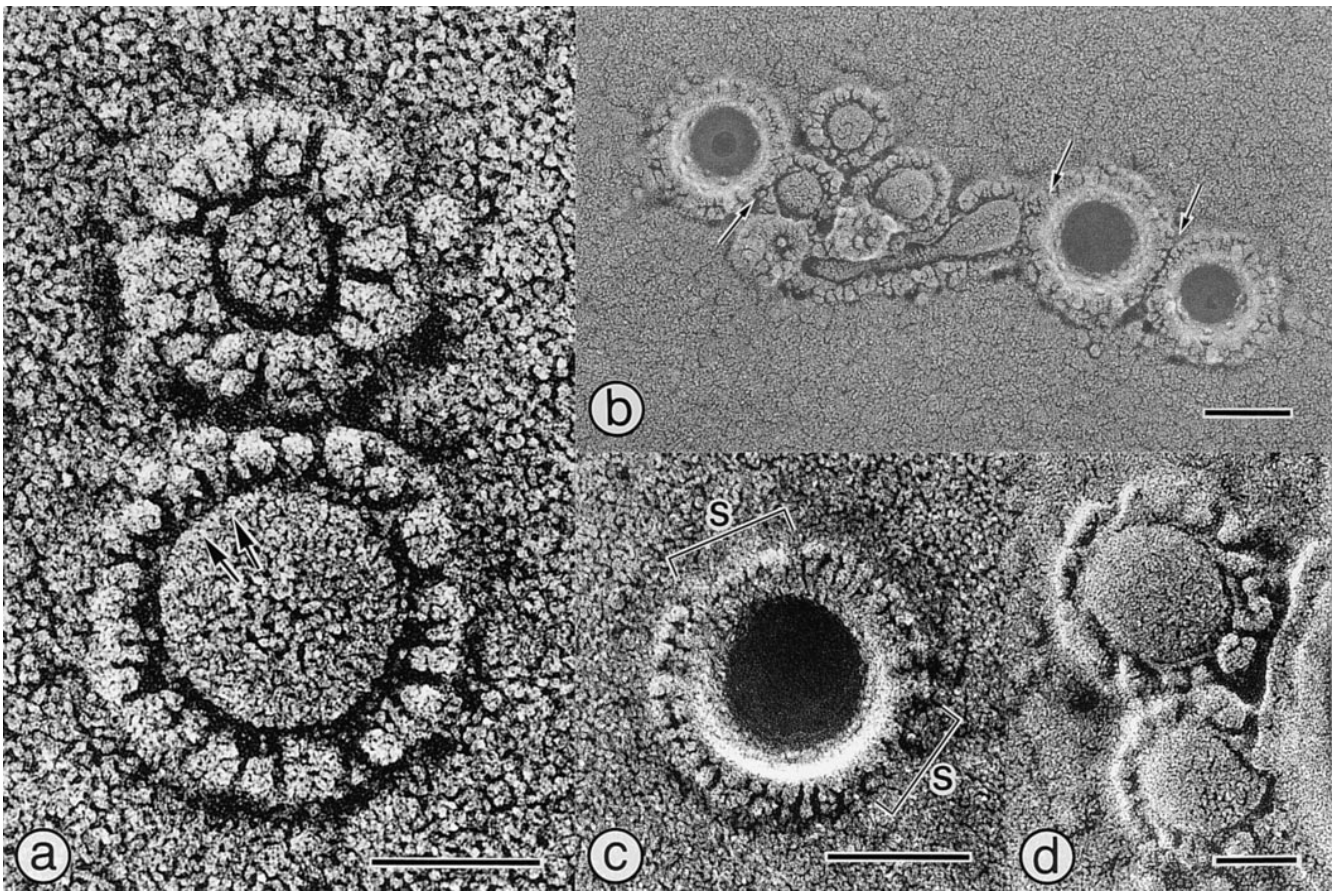

Figure 3. Influenza viruses incubated at pH 5.0 and 23°C for 30 s before freezing. (*a* and *d*) The appearance and the height of the spikes are unchanged from those at neutral pH. Arrows indicate stalked spikes grouped together. (*b*) Spikes at contact sites of virions (*arrows*) are apparently shorter than the other spikes. (*c*) In rare cases, short spikes (indicated by *s*) are observed on solitary virions. Bars: (*a*, *c*, and *d*) 50 nm; (*b*) 100 nm.

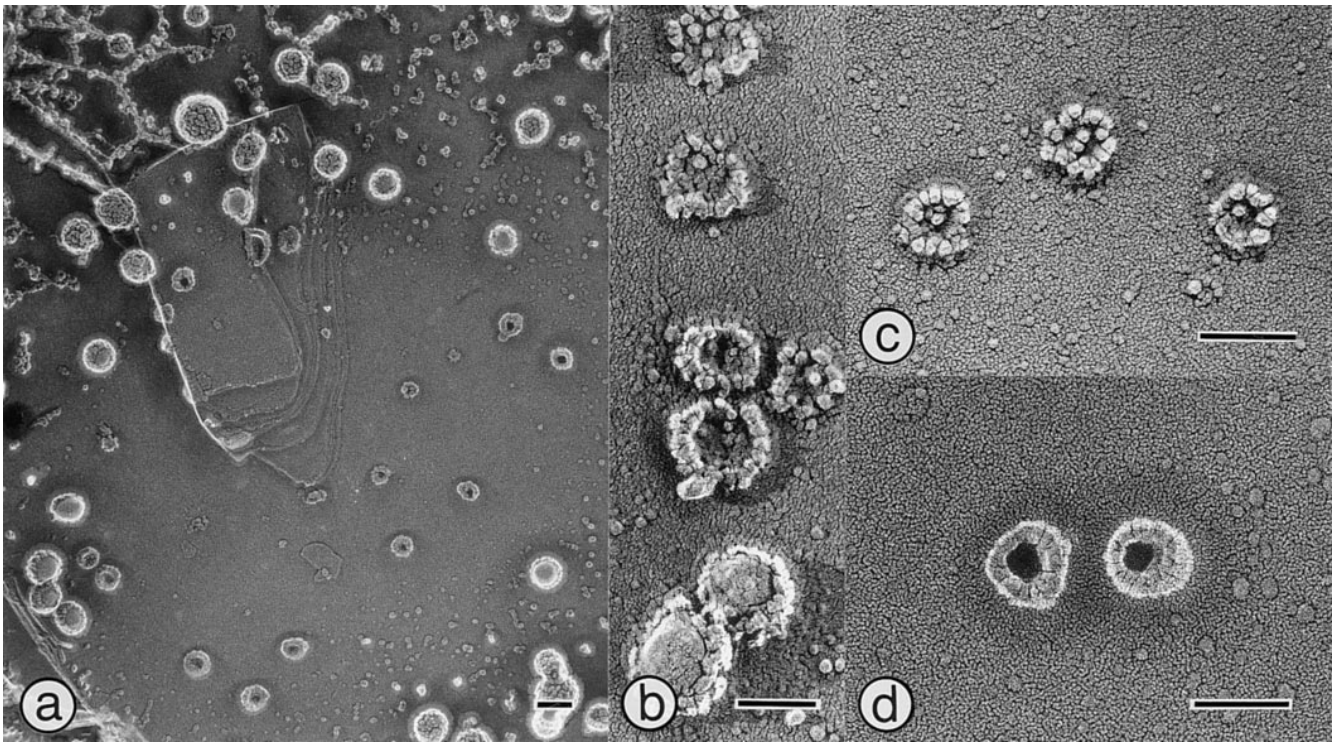

Figure 4. Appearance of frozen influenza viruses on the surface of mica. (*a* and *d*) Viruses incubated for 30 s at pH 7.4 and 23°C were mixed with mica flakes and frozen for replication. (*b* and *c*) Viruses similarly processed at pH 5.0. For explanation see Results. Bars, 100 nm.

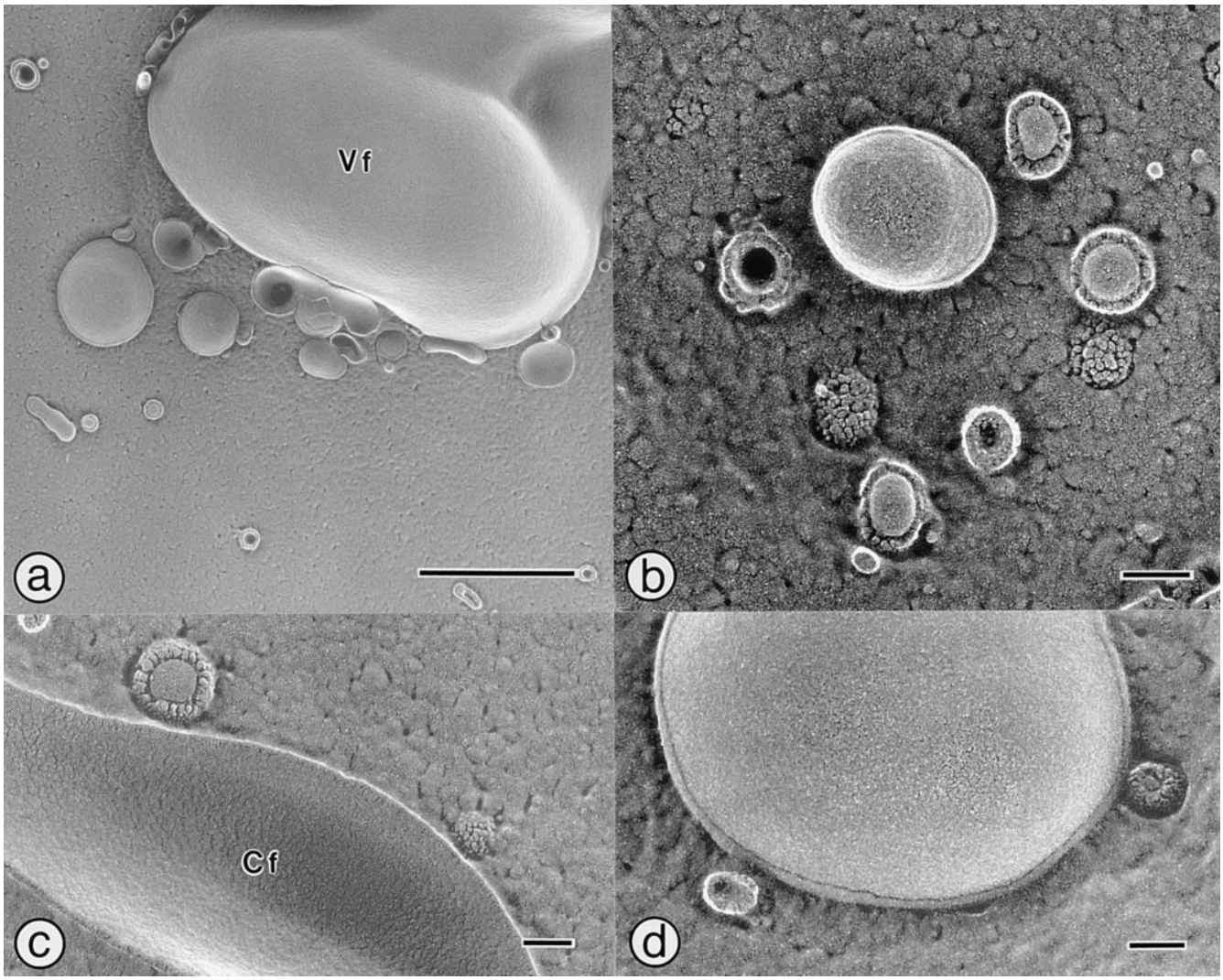

Figure 5. Influenza viruses mixed with liposomes at pH 7.4 and 23°C, and incubated for 30 s before freezing. (*a–d*) Note that fractured convex faces (*Vf*) of the liposomes appear very smooth and velvety. Virions adhering to the surface of the liposomes are evident. *Cf*, concave face of liposome. Bars: (*a*) 1 μm; (*b–d*) 100 nm.

and *d*) and the fractured concave faces (Fig. 5 *c*) of the liposomes appeared very smooth and velvety and free from any blisters or warts. It was not possible to observe glycophorin on fractured liposomal faces as IMPs or any other microscopic structural feature. In addition, the liposomes alone at pH 5.0 showed the same velvety face as those at pH 7.4 (see the concave faces shown in Fig. 10 *g*).

Viruses and Liposomes at Acidic pH

In contrast to the results obtained at pH 7.4, after only a 19-s incubation at pH 5.0 and 23°C, many viruses were adsorbed to the surface of the liposomes as if competing for sites (Fig. 6 *a*). However, an extremely interesting finding was the presence of blisterlike or wartlike small protrusions, each 10–20 nm in diameter, on the fractured convex face of the liposomal membrane. These protrusions were found alone or in triangular or rectangular arrangements. However, the most interesting configuration formed by the protrusions was a ringlike heptagon. These heptagons often had an additional centrally located protrusion. In Fig. 6 *a*, four heptagons are evident in the upper right region of the liposome face. Three of them have additional protrusions in the center. The outer diameter of each heptagon was typically about 100 nm, roughly corresponding to the diameter of the virus. The distance between the protrusions varied, but was usually ~40–50 nm. The area circumscribed by the heptagon on the face of the liposome appeared to show slight inward depression.

As shown in Fig. 6 *b*, the viruses were not of uniform size, but both large and small ones coexisted in the same sample. On the bottom of the concave fracture face of the largest liposomal membrane, another heptagon arranged in a ringlike configuration can be seen. This time, however, it is composed of seven pits on the vertices and a centrally located pit. Judging from the size of the heptagon, it is undoubtedly complementary to the previous heptagon composed of protrusions on the convex face. On closer observation, two virions can be seen directly below the polygonally arranged pits in Fig. 6 *b* (*arrows*). Judging by the

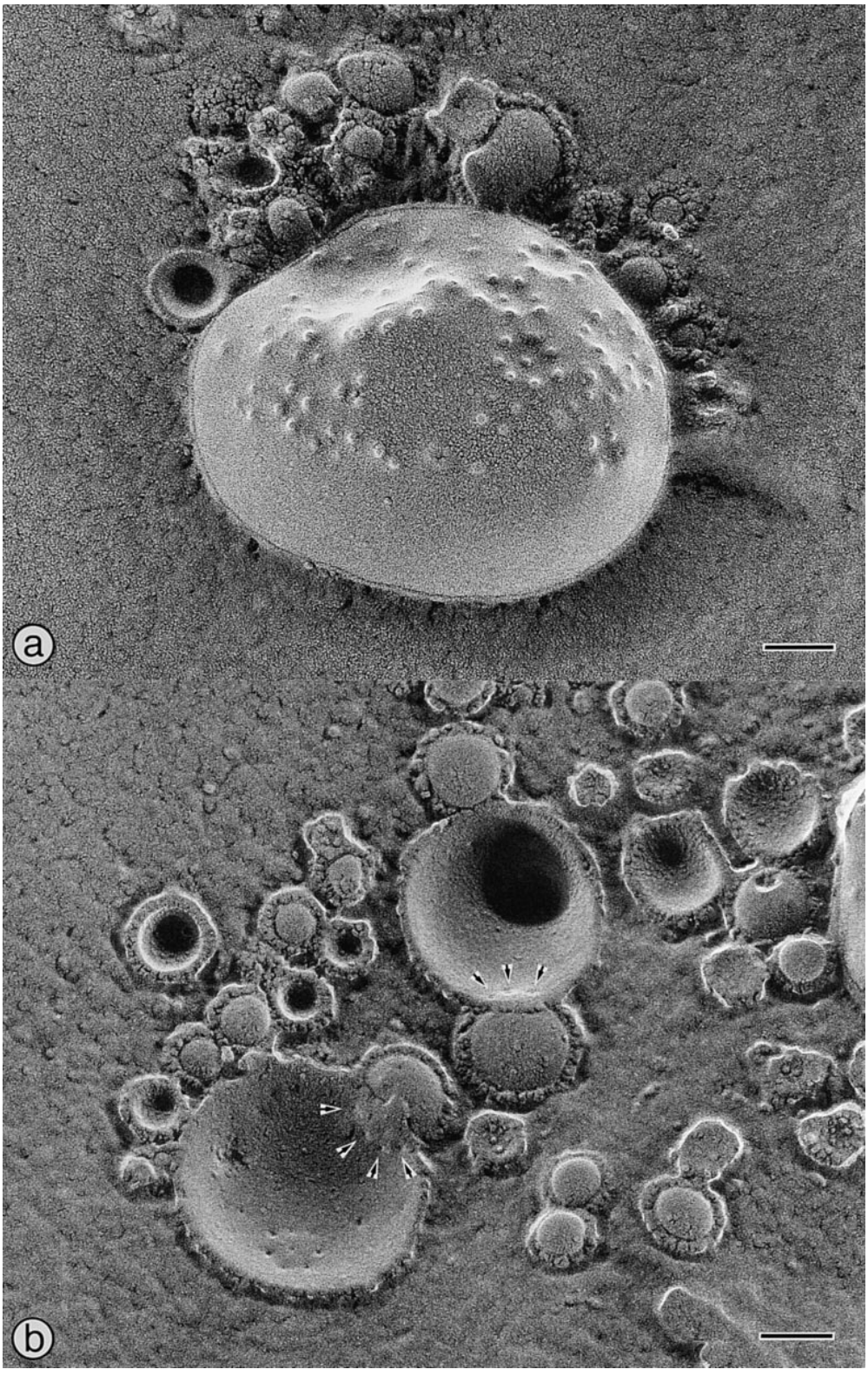

Figure 6. Influenza viruses and liposomes at 19 s after acidification at pH 5.0 and 23°C. (*a*) Adsorption of viruses onto the liposome surface. The convex face of the liposome membrane is exposed. Many small protrusions 10–20 nm in diameter are evident. They are observed singly as well as in triangular, rectangular, and even pentagonal formations. However, the most interesting configuration is a heptagon with an occasional centrally located protrusion. (*b*) Two liposomes with their concave fracture faces exposed. On the lower liposomal face a heptagon composed of seven small pits with a centrally located pit is present. Judging from the diameter of the pit heptagon, it is clear that it is complementary to the heptagon composed of seven small protrusions. Two large viruses are observed just below the pits arranged in a polygonal manner (*arrows*). These pits delineate the contour of viral spikes. Some pits also exist solitarily. Bars, 100 nm.

formation of these pits, it seems clear that the pits and protrusions on the faces of the liposomes are actually produced by the action of the virus and possibly by HA spikes. We also observed that the area circumscribed by the pit heptagon on the concave face appeared to be pushed inward slightly. Some pits also existed solitarily on the concave face.

Structures of Small Protrusions and Pits

Before discussing the role of the protrusion and the pit as the "fusion apparatus," we must clarify their conformation in membranes. For example, "inverted micelles" have been reported on the fracture faces of artificial membranes (Cullis et al., 1979; for review see Verkleij, 1984).

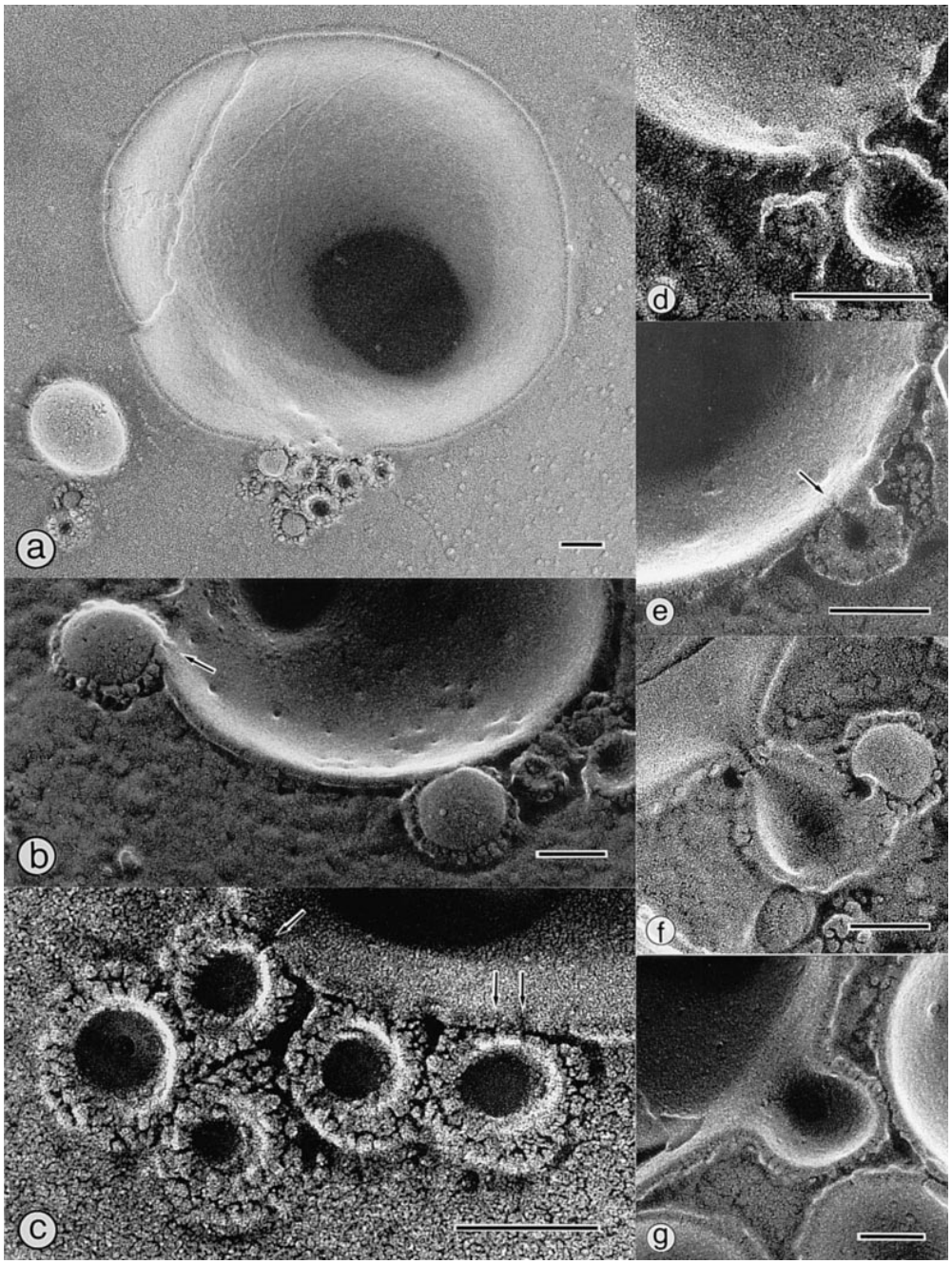

Figure 7. Influenza viruses and liposomes 19 s after acidification at pH 5.0 and 23°C. (*a*) Virions of smaller size are observed directly below a liposome with its concave face exposed. There are many solitary pits just above the virions. Note that no pits can be detected on the remainder of the liposome membrane. (*b*) Many solitary pits and a few rectangularly grouped and even pentagonally grouped pits are present on the concave face. Around the pit indicated by an arrow, the viral and liposomal membranes have connections suggestive of fusion between the two. (*c*) Cross-fractured viral and liposome membranes. Arrows indicate slits between the viral and liposomal membranes. (*d*) Five solitary pits are present on a concave face. One has turned into a narrow slit bridging the liposome and a virus. (*e*) Observed from just above (*arrow*), the slit is seen to consist of a narrow channel ~4 nm in diameter. (*f* and *g*) The slit appears to widen until an omega-shaped fusion neck is formed. Bars, 100 nm.

These micelles present a structural appearance similar to the small protrusions we observed on convex faces. Here, we define a microprotrusion as having a bilayer arrangement of lipid molecules continuous with the rest of the membrane.

Since the small protrusions on convex faces and the small pits on concave faces had the same polygonal arrangement, it is apparent that they result from the same membrane domains and are complementary to each other. In addition, the protrusions were observed only on convex faces and the pits only on concave faces. These facts indicate that if the protrusions and pits are combined they reconstruct small bendings of the continuous lipid bilayer, which protrude outwardly.

Direct evidence for this interpretation is shown in the large fractured face of a liposome in Fig. 8 *b.* The outer line of the liposome, labeled *M*, represents the hydrophilic surface of the outer leaflet of the unit membrane. The inner line labeled *L* delineates the hydrophobic interior of the membrane, which at its closest point to the outer line might roughly be considered to represent the outer leaflet of the unit membrane. The outer and inner lines of the convex liposome membrane are observed to run parallel with each other in close apposition. They are parallel even at the site of the projection labeled *Pr*, where the liposome membrane is fusing with a virus on the left.

Therefore, we consider that the protrusions on convex faces and the pits on concave faces correspond to the

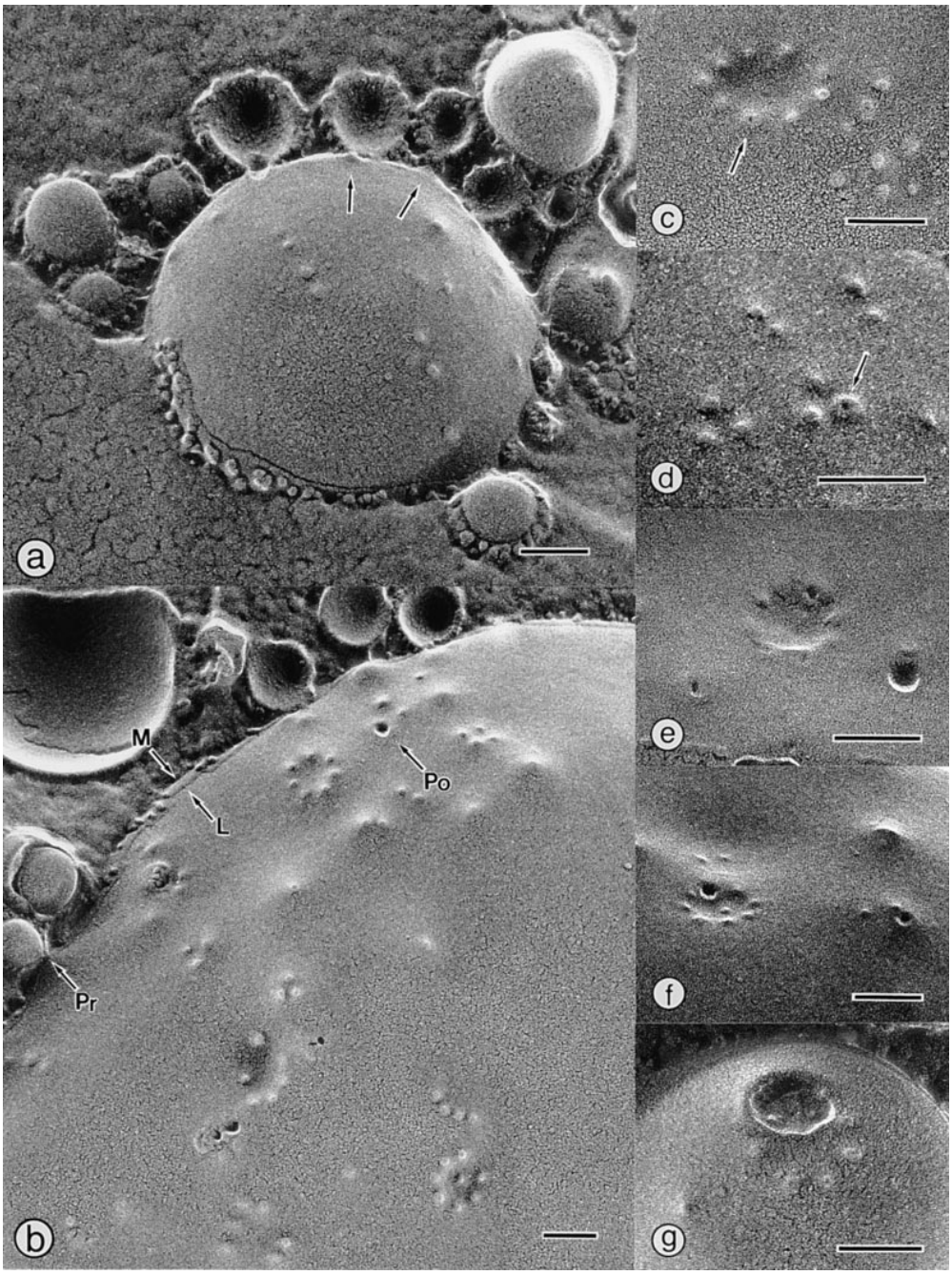

Figure 8. Influenza viruses and liposomes 19 s after acidification at pH 5.0 and 23°C. (*a*) Several solitary protrusions present on the convex face of a liposome. Four viral E-face membranes are adherent to the surface of the liposome in a shape reminiscent of micropinocytosis. Necks or "fusion rings" apparently connected with solitary protrusions (*arrows*) can also be observed. (*b*) A variety of heptagonally, triangularly, or rectangularly arranged groups of small protrusions are evident on the broad convex face of a liposome. The arrow labeled *Po* indicates fusion rings apparently occupying the site of a protrusion in the vertex of a triangle. For explanations of the arrows labeled *M*, *L*, and *Pr*, see Results. (*c*) Nine protrusions arranged in a polygonal manner. Note that each protrusion differs slightly in diameter. The arrow indicates the largest, which has a hole <4 nm in diameter in the center. (*d*) A hole is also evident in the center of a protrusion in a triangular group. Again, the hole is found in the largest protrusion. (*e–g*) Fusion rings associated with protrusions showing a polygonal arrangement. The rings appear to have developed from holes in the centers of the protrusions. Bars, 100 nm.

bends of a continuous lipid bilayer, and not to the lipidic particles proposed for fusion between model membranes. We refer to this structure as a microprotrusion of the lipid bilayer or a microprotrusion of the membrane.

Further evidence for the structure of the microprotrusion is given in the section entitled Fusion between HA-equipped Liposomes.

Fusion Events on Concave Faces

In Fig. 7*a*, a cluster of relatively small viruses is evident directly below a liposome with its concave face exposed. On the concave face, just above the viruses, several solitary pits can be seen. It is noteworthy that no pits are present on the other parts of the concave face of this liposome. We surmise that the solitary pits are also generated by the activity of viruses, mainly of smaller size.

Fig. 7 *b* shows the concave face of a liposome with pits in various arrangements. Many are solitary, but some are grouped rectangularly. Pentagonally arranged pits are also present. Around the pit indicated by the arrow, the viral and liposomal membranes show connections suggestive of fusion between the two membranes.

Fig. 7 *c* is a high magnification micrograph of cross-fractured viral membranes and a liposome membrane. Many slits or connections between the viral and liposomal membranes are clearly observable (*arrows*). The virus on the far right may be connected to the liposome by two slits.

On a favorable fracture plane shown in Fig. 7 *d*, several pits are observable on the concave face. However, one of

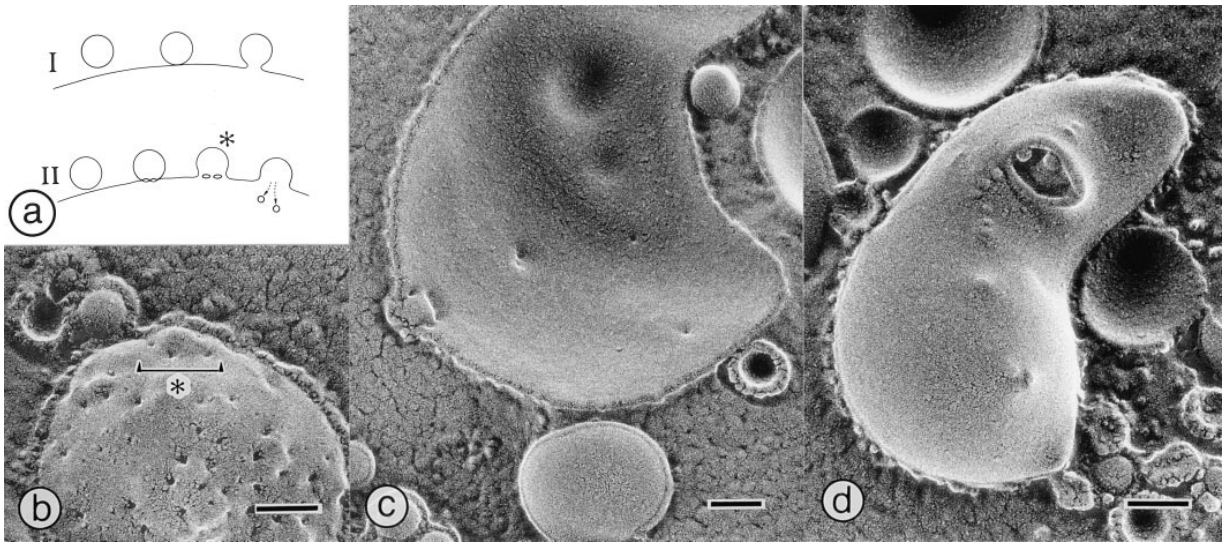

Figure 9. Influenza viruses and liposomes 30 s after acidification at pH 5.0 and 23°C. (*a*) A schematic drawing of two series of fusion events. We refer to the series in *I* as single-point fusion, and to that in *II* as multi-point fusion. (*b*) Many large holes are seen to surround membrane protrusions on the convex liposomal face. The protrusion marked with an asterisk apparently corresponds to the asterisked drawing in *a.* (*c*) A liposome with a concave face exposed is shown. Two or three solitary pits are present in the central part. On the left, pits forming a circle are evident. This part corresponds to the labeled drawing as observed from underneath. (*d*) The convex face of a liposome. A fusion ring containing two vesicles is evident. These vesicles are apparently derived from the liposome membrane, as depicted in the lower right corner of *a.* Bars, 100 nm.

them appears to have been transformed into a narrow slit bridging the liposome and the virus. When observed from just above, as shown in Fig. 7 *e* (*arrow*), the slit was seen actually to consist of a narrow channel ~4 nm wide. These slits were thought to correspond to the initial fusion pore, and would widen until omega-shaped fusion necks were formed between the virus and liposome (Fig. 7, *f* and *g*).

Fusion Events on Convex Faces

On the convex face shown in Fig. 8 *a*, several solitary protrusions can be seen. Four viral membranes with exposed E-faces adhere to the surface of the liposome in a shape reminiscent of micropinocytosis. Fusion necks can also be observed, apparently connected to solitary protrusions (*arrows*).

A broad plane of the convex face of a liposome is shown in Fig. 8 *b.* Here and there, protrusions arranged in heptagonal, triangular, or rectangular configurations are evident. Fusion rings can also be observed. There appears to be one at the vertex of a triangle where a protrusion should have been located (arrow labeled *Po*).

A polygonal ring composed of nine protrusions is shown in Fig. 8 *c.* The diameter of each protrusion differs slightly. The largest one indicated by an arrow has a tiny hole <4 nm in diameter in the center. A hole can also be seen in the center of one protrusion which forms part of a triangular arrangement in Fig. 8 *d* (*arrow*). The diameter of this hole is apparently larger than the others. Upon observing the fusion rings associated with polygonally arranged protrusions on the convex faces shown in Fig. 8, *e–g*, we concluded that the fusion rings had formed from small holes located in the centers of the microprotrusions.

Sequence of Fusion Events

Therefore we suggest that the sequence of events during the process of fusion may be as follows: (*a*) A connection between two membranes is made via microprotrusions which may form from either side. (*b*) The initial fusion pore, observed as a small hole and a narrow slit, is formed in the center of each microprotrusion. (*c*) The initial fusion pore expands to become visible as a larger fusion ring or a larger fusion neck. (*d*) On a single virion, fusion may proceed in parallel on many of the microprotrusions that form polygons.

If this tentative hypothesis is true, we should be able to observe the stages of the theoretical sequence of fusion events depicted in the diagram shown in Fig. 9 *a.* We refer to the sequence of fusion events depicted in the upper model (Fig. 9 *a*, *I*) as single-point fusion, and that depicted in the lower model (Fig. 9 *a*, *II*) as multi-point fusion. Relatively small virions appeared to undergo single-point fusion, as in Fig. 7, *a*, *d*, *e*, and *f*, whereas larger virions underwent multi-point fusion, as in Fig. 6 *b.* The sequence of fusion events for single-point fusion has already been shown in Fig. 7, *d–g.* This sequence could also be observed in the case of multi-point fusion in a three-dimensional manner.

On the convex liposomal face in Fig. 9 *b*, many large holes surrounding membrane protrusions are present. The protrusion marked with an asterisk apparently corresponds to the stage marked with an asterisk in Fig. 9 *a*, as seen from the outside. In the lower left corner of the concave face of the liposome in Fig. 9 *c*, several pits aligned on a circle were seen. This appears to correspond to the asterisked stage in Fig. 9 *a* as observed from underneath. The fracture shown here passed through the concave face of

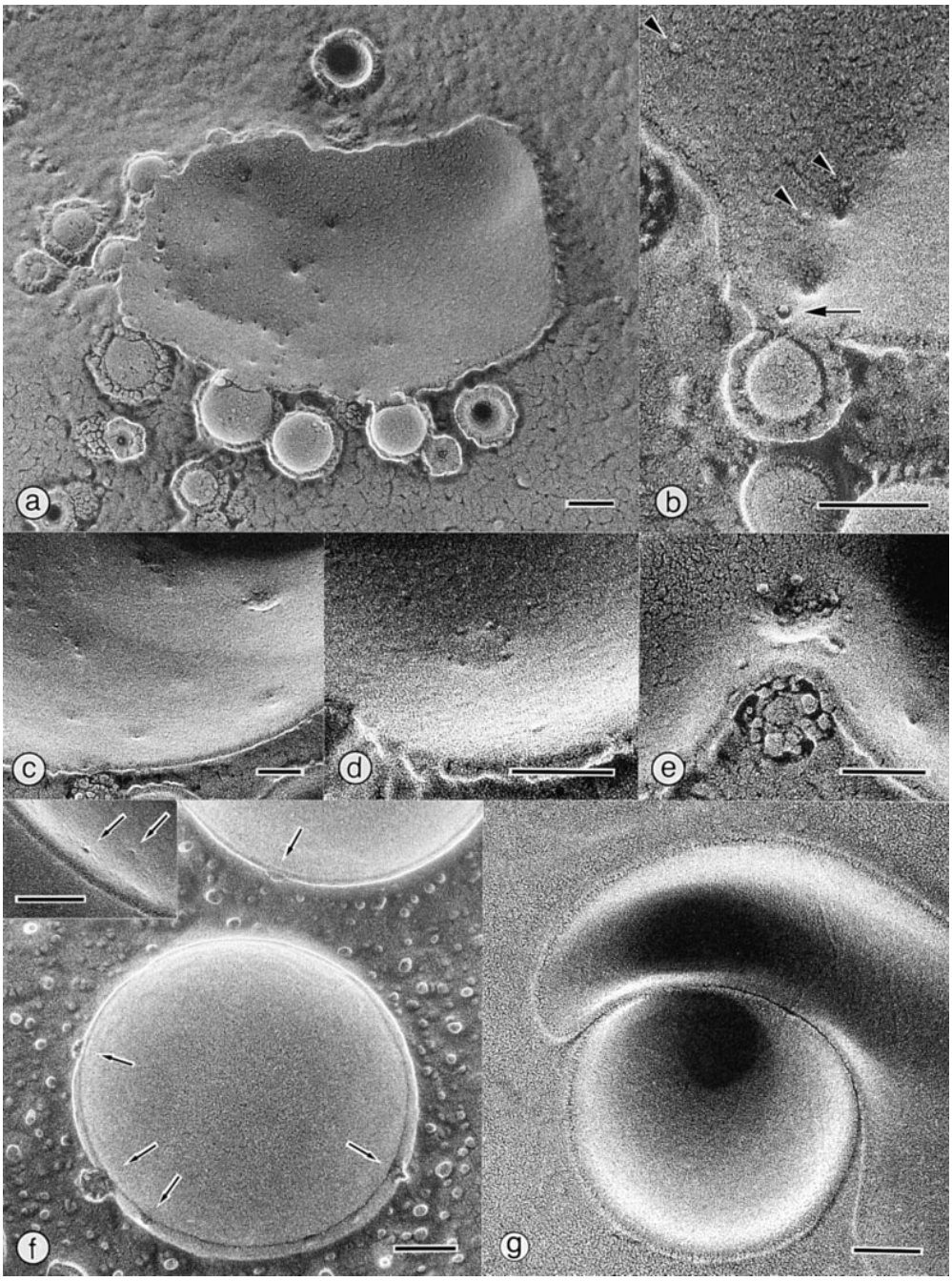

Figure 10. Influenza viruses and liposomes (*a–e*), and HA rosettes with liposomes 30 s after acidification at pH 5.0 and 23°C (*f* and *g*). (*a*) Solitary pits on a concave liposome face. Some of them contain IMPs. (*b*) The arrow indicates a pit containing a very distinct IMP ~10 nm in diameter. Note that a virus is positioned directly below the pit. Arrowheads indicate IMPs that are free from pits. Three larger pits contain no IMPs. (*c* and *d*) Pits forming a polygon are also occupied by IMPs. (*e*) In terms of size, there are two kinds of IMPs. The IMP at the neck of the depression is larger than the one at the bottom. The measured diameter of the IMP at the bottom is about 6 nm. (*f*) Arrows indicate HA rosettes of various sizes on the outer surface of the liposome. Note that no protrusions are present on the convex face. (*f*, *inset*) Arrows indicate two IMPs ~10 nm in diameter on the concave face of a liposome incubated with HA rosettes in acidic buffer for 30 s. No pits can be seen on the concave face. (*g*) Liposomes alone frozen at pH 5.0. Although the magnification of this figure is larger than that of the inset in *f*, no IMPs can be observed. Bars, 100 nm.

the liposomal membrane and continued with the viral membrane at the locations of the pits, then again continued with the liposomal membrane. If these pits were to fuse and dilate, the central part of the membrane would become isolated in the form of a vesicle, as shown in the lower right corner of Fig. 9 *a.* In Fig. 9 *d*, two isolated vesicles can be observed in the fusion ring. Thus we surmise from the morphological evidence that fusion actually occurs between the viral and liposomal membranes, using tiny pits and protrusions as the fusion apparatus.

Nature of IMPs on Concave Faces

The concave fracture face of a liposome membrane fusing with viral particles at 30 s after reduction of the pH of the reaction mixture is shown in Fig. 10 *a.* Careful scrutiny reveals the presence of many pits on the plane. Surprisingly, however, each pit is occupied by an IMP. Originally, the liposome membranes had no IMPs (Fig. 4). Therefore, these particles present on the concave fracture face appear to have issued from viral membranes as a consequence of pH reduction.

Four pits are evident on the concave face of the liposome shown in Fig. 10 *b.* Three of them have no particles in the center. However, the pit indicated by an arrow has a very distinct IMP ensconced in the center. A virus is positioned directly below the pit containing the particle, suggesting that the particle itself could in fact be a part of HA

delivered from the virus. IMPs free from pits were also observed (*arrowheads*). The pits that did not contain IMPs were larger than those that contained a particle.

Pits forming a polygon were also sometimes occupied by IMPs, as shown in Fig. 10, *c* and *d.* In Fig. 10 *e*, there are several IMPs at the neck of a membrane depression. Since some IMPs on the concave face were free from pits, particles at the neck seemed to emerge from the pits and travel outwardly along the interior of the liposomal membrane away from the original polygonal area. Although IMPs were also located at the bottom of the depression, the particles at the neck were ~10 nm in diameter and larger than those at the bottom. Measurement revealed that the smaller particles were similar in size to the IMPs observed on the viral E-face membranes.

To explore the nature of the IMPs on the fractured face of liposomal membranes, we purified HA rosettes from intact influenza virus. The HA rosettes were mixed with liposomes at neutral pH, and incubated for 30 s at pH 5.0 and 23°C, followed by rapid freezing for replication. As shown in Fig. 10 *f*, the HA rosettes were observed as aggregates of various sizes adhering to the outer hydrophilic surface of the liposome (*arrows*). No protrusions could be found on the convex face, either solitarily or in the form of polygons. Furthermore, no pits were evident on the concave face.

We examined the possibility that HA rosettes might penetrate into the membrane interior to form IMPs. Observation of the reverse side of the fracture face confirmed the existence of such IMPs, as shown in the inset of Fig. 10 *f* (*arrows*). The diameter of the particles was ~10 nm, resembling that of the larger IMPs ensconced in the pits. As shown in Fig. 10 *g*, no IMPs were observed in the concave faces of two liposomes frozen alone at pH 5.0. Therefore, there is good evidence to suggest that the particle ensconced in the pit is part of HA that has gained enough hydrophobicity at pH 5.0 to penetrate into the lipid membrane core.

Fusion between HA-equipped Liposomes

In the same samples in which we observed fusion events between viruses and liposomes, some liposomes had already acquired HA spikes on their surfaces as a result of fusion with viruses. The liposomes equipped with HA appeared to fuse with the same sequence of morphological intermediates as that observed between viruses and liposomes. Perhaps it would be appropriate here to describe briefly the observations we made concerning fusion between HA-equipped liposomes. We were able to obtain some new findings due to the large radii of the two fusing liposomes.

The etched surface of the liposome shown in Fig. 11 *a* (30 s after acidification) appears very smooth, without any incorporated material. However, the surface of the liposome in Fig. 11 *b* (same sample as that shown in Fig. 11 *a*) has many projections, which would be HA spikes transferred from the viruses by fusion. A liposome densely covered by the projections is also shown in Fig. 11 *c.*

On convex liposomal faces (Fig. 11 *d*), protrusions were also induced, but no regular heptagonal arrangement of protrusions was observed, though a somewhat ringlike arrangement of larger size could be detected. Three fusing liposomes are shown in Fig. 11 *e.* Two of them, with concave faces exposed, show a narrow channel <10 nm wide at the fusion point (*arrow*). A low magnification view of two fusing liposomes is shown in Fig. 11 *f.* The protrusions, arranged in a ringlike manner on the convex face, adhere to the covering liposomal concave membrane at the vertices of the protrusions. Observed from the outside (Fig. 11 *g*), the points of adhesion were bridges between the two fusing convex faces of the liposomes, which also clearly demonstrated the multi-point type of fusion shown in the asterisked drawing in Fig. 9 *a.* Fig. 11 *h* shows two fusing liposomes with their concave faces exposed. In the center, two half membranes displaying a classical fused membrane–like junction have been fractured perpendicularly. The junctional profile is associated with three pits, which are paired with pits of equal size across the junction (*arrows*). If we imagine the complementary convex faces superimposed upon these concave faces, it becomes convincing that the connections between the two membranes are actually formed via membrane microprotrusions from both sides.

On a favorable replica like that shown in Fig. 11 *i*, pits and protrusions are seen to form a single polygon. Tiny holes are evident in the center of the protrusions (*short arrows*). Around the hole indicated by a long arrow, two half membranes, the upper concave and the lower convex, appear to be connected to each other. Two or three small pits containing IMPs were observed on the concave face of the upper liposomal membrane. These IMPs were presumed to have issued from the lower liposomal membrane. It seemed most probable that there would be protrusions at exactly the corresponding locations on the convex face directly underneath the IMPs. Also, the convex face complementary to the concave face bearing the pits would also have protrusions at the sites directly above the pits. Thus we conclude that a single IMP on one side of two fusing membranes can induce microprotrusions in both opposing membranes.

In Fig. 11 *j*, we can see examples of events occurring throughout the process of fusion between liposomes, exactly the same as those observed between viruses and liposomes. (*a*) A connection is made via microprotrusions from both sides. (*b*) An initial fusion pore forms as a perforation in the center of each microprotrusion. (*c*) The pores widen to form fusion rings. Thus in the case of fusion between liposomes, the microprotrusions and the pits also constitute the fusion apparatus.

Discussion

Asymmetrical Distribution of Protrusions, Pits, and IMPs

In this study, we clarified the structure of microprotrusions of the lipid bilayers between fusing influenza virus and liposomes, which were observed as small protrusions on the fractured convex faces and as small pits on the concave faces. Two previous studies have investigated HA-mediated fusion using quick-freezing replica techniques (Knoll et al., 1988; Burger et al., 1988). In these studies, particles, pits, and invaginations were observed on target liposomal

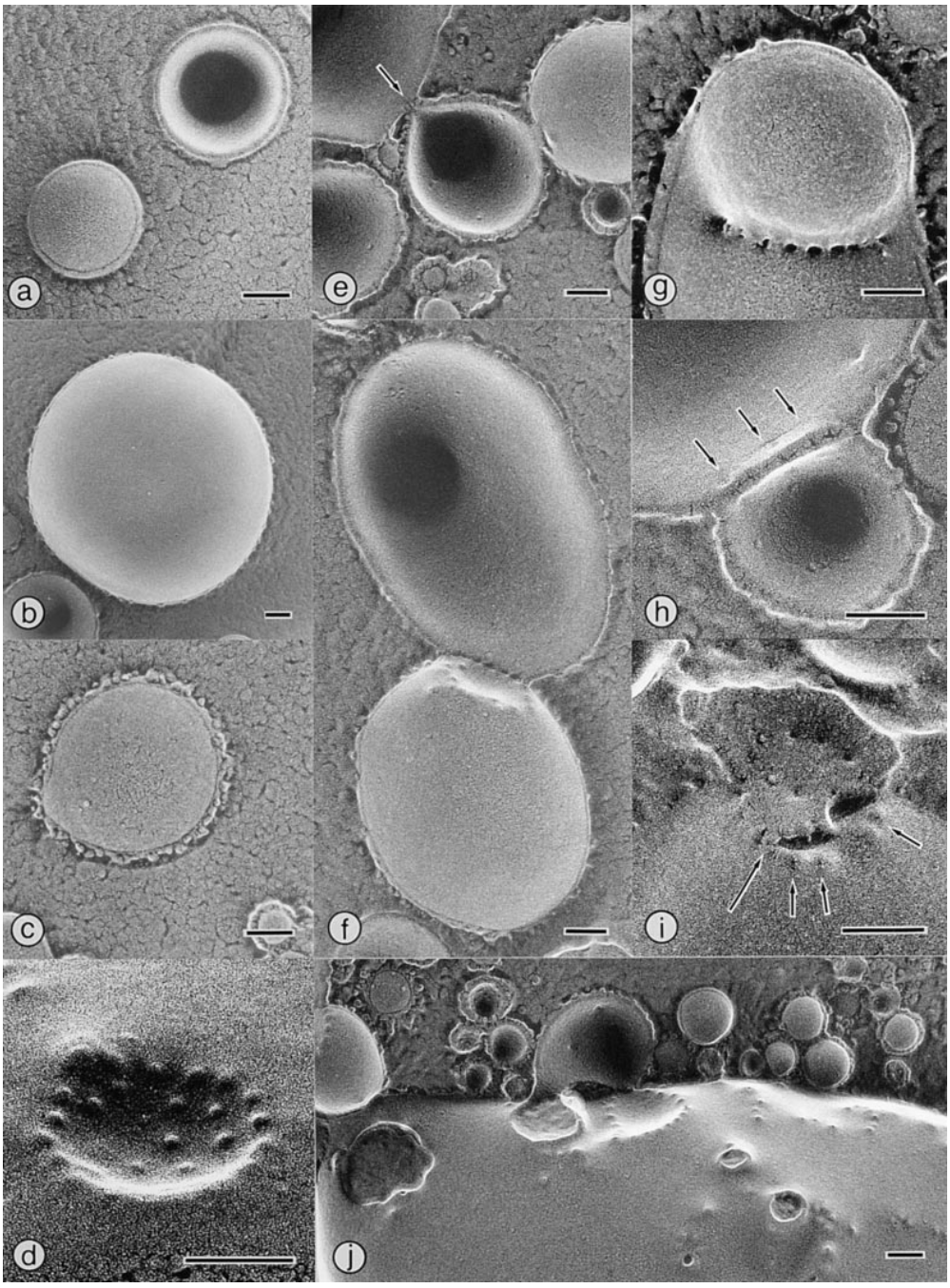

Figure 11. Morphological sequences of fusion events between HA-equipped liposomes in a virus–liposome mixture 30 s after acidification at pH 5.0 and 23°C. For explanation see Results. Bars, 100 nm.

membranes, which were apparently similar to those we observed.

Knoll et al. (1988) studied the fusion of liposomes with the plasma membrane of cultured cells infected with influenza virus. After a 30-s incubation at pH 5.0 and 37°C, they observed well-defined IMPs and pits on the concave and convex fracture faces of the liposomes and on those of the plasma membrane. These particles were thought to be lipidic in nature, based on the assumption that viral spike-protein particles would have appeared exclusively on the concave fracture face of the liposome.

We think that our results are different from those of Knoll et al., since they reported a symmetrical distribution of small protrusions, pits, and large IMPs on the concave and convex faces, whereas we found the small protrusions exclusively on the convex face, and the pits and IMPs exclusively on the concave face.

An experiment similar to ours was performed previously by Burger et al. (1988). They quickly froze influenza virus and viral receptor–containing liposomes and processed them for EM. At pH 7.4 and 37°C, the viruses did not fuse with the liposomal membrane, but induced protrusions 35–60 nm in diameter predominantly on the convex liposomal fracture face. Invaginations complementary to the protrusions were predominant on the concave face. In the center of each protrusion, they observed a well-defined particle 9–14 nm in diameter. They regarded the particle as a local point–contact site between the viral and

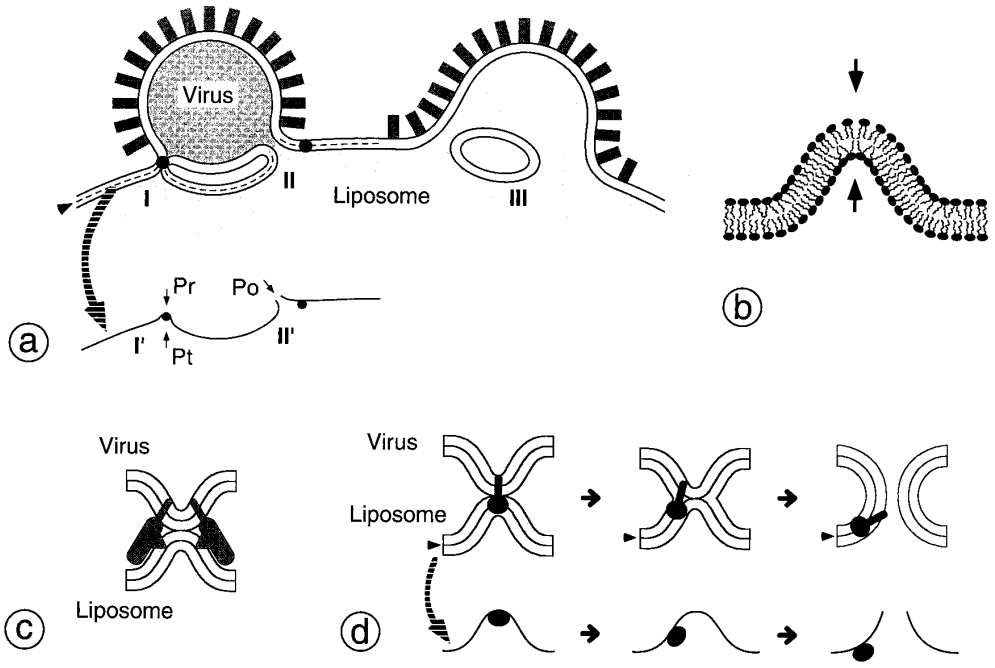

Figure 12. Schematic drawings of HA-mediated fusion mechanisms. (*a*) The proposed sequence of fusion events. Upon acidification, the viral membrane and the liposomal membrane are strongly connected by HA protein. The hydrophobic parts of HAs that have penetrated into the liposome are depicted as small solid circles at *I* and *I′* (the hydrophilic parts of HA are not drawn). At site *I*, both membranes are bent to form a microprotrusion of the lipid bilayer. On the fractured interface (labeled *I′*), this part appears as a small protrusion (arrow labeled *Pr*) on the convex liposomal face, and as a pit containing an IMP (arrow labeled *Pt*) on the concave face. At the microprotrusion, an aqueous pore forms through the two membranes (site *II*). On the corresponding fractured interface (labeled *II′*), a larger protrusion with a small pore at its center (arrow labeled *Po*) is observed on the convex liposomal face. Through the dilation process, fusion pores expand into distinct fusion sites. A multi-point fusion on a single viral particle forms an intervening membrane (labeled *III*) after growth of the fusion sites. (*b*) A sectioned profile of the microprotrusion. The diameter of the microprotrusion is only 10–20 nm. For details, see Discussion. (*c*) A model of the fusion site surrounded by multiple HA spikes. We observed no spike structures closely surrounding the fusion site (*shaded objects*). (*d*) Schematic drawings of a microprotrusion of the lipid bilayer with an IMP at its center. The centrally located HA spikes, anchored to both the apposing membranes as IMPs, may tug out the membranes to form microprotrusions of the lipid bilayer. (*Top*) The small black objects denote the hydrophobic parts of HA anchored to the membranes (hydrophilic parts are not drawn); the rods denote the transmembrane domains of HA, whereas the circles denote parts of HA which have penetrated into the liposome. (*Bottom*) Changes in the fractured interface, corresponding to the changes in the microprotrusion shown in the upper panel. See also Discussion.

liposomal membranes at neutral pH. At pH 5.4 and 37°C, they observed many IMPs on the concave liposomal fracture face. Because IMPs with the same appearance were present exclusively on the E-face of intact viruses, they interpreted these IMPs to be representative of viral spike protein.

Contrary to the observation made by Burger et al., we found that at neutral pH the virus did not induce any structural change on the liposomal membrane; neither protrusions on the convex faces nor invaginations on the concave faces were observed. Therefore the 9–14-nm particle that Burger et al. observed at neutral pH on the liposomal convex face may be an entirely different structure from the microprotrusion we observed.

We found two kinds of IMPs on the concave face of liposomes processed at pH 5.0 with the virus. The smaller IMPs, ~6 nm in diameter, are similar to those on the viral E-face, which may correspond to the membranous segments of HA, and which are thought to be unrelated to the fusion intermediate. On the other hand, the larger ones, ~10 nm in diameter, often appeared to be ensconced in the pit, and it is noteworthy that the IMPs contained in the pits were positioned directly above the viruses bound to the liposomes. Therefore we suggest that the larger particle may be a portion of the HA protein that includes the fusion peptides, and may play a critical role in the fusion event.

Fusion Pathway via the Microprotrusion of the Lipid Bilayer

We concluded that the microprotrusion of the lipid bilayer is the intermediary membrane structure that forms during HA-induced fusion. A schematic drawing of the proposed sequence of events is shown in Fig. 12 *a.* A drop in pH causes the hydrophobic fusion peptide and some other part of HA to penetrate into the lipid bilayer of the liposome, connecting strongly and bending the apposing membranes. The portion of HA that penetrates into the interior of the liposomal membrane is depicted as small solid circles in the figure. When observed using the freeze-fracture technique, this part would appear as a small protrusion on a convex liposomal face, while on a concave face, it would be seen as a pit containing an IMP (as shown in Fig. 12 *a*, *I* and *I′*). We believe that each small protrusion with no observable hole contains an IMP, and that the fusion intermediate must be a lipid–protein complex.

As fusion proceeds, an aqueous pore must form between the viral membrane and the liposomal membrane. If we observe the pore site on the convex liposomal fracture face, a larger protrusion with a tiny hole in the center may be seen, while on the concave face, we should see a pit of small diameter containing no IMP (Fig. 12 *a*, *II* and *II′*).

In the course of the expansion of fusion sites, fusion pores may assume various diameters, as shown in the right

corner of Fig. 12 *a.* Since the fusion pores may form at multiple sites on a single viral particle, growth of the fusion sites would produce an intervening membrane with a complex morphology.

As we have described in Results, all the membrane structures discussed here were actually demonstrated by our EM observations.

Initial Fusion Pore

In patch-clamp studies of fusion between HAb-2 cells and RBC, Spruce et al. (1989) estimated the diameter of the initial fusion pore to be <4 nm, and this was suggested to subsequently expand. Sarkar et al. (1989) studied the redistribution of a water-soluble fluorescent probe, NBD-taurine, from RBC to HA-expressing cells (GP4F), and also proposed that the initial fusion pore is no larger than 4.5 nm. The measured diameter of the smallest hole in the protrusions which we observed was <4 nm. We also observed a narrow slit <10 nm wide, bridging the concave faces of the virus and liposome. Our observations are consistent with the results of Spruce et al. and Sarkar et al., and we consider that the smallest hole and the narrow slit are direct evidence for the initial fusion pore.

Architecture of the Fusion Intermediate

A sectioned profile of the microprotrusion is shown schematically in Fig. 12 *b.* To our knowledge, no previous reports have described such a small membrane curvature as that of the microprotrusion we observed (10–20 nm). It should be noted that the thickness of a lipid bilayer is usually 4–5 nm. Because of the remarkably small diameter of the microprotrusion, the packing of lipid molecules in the top of the outer leaflet would be quite loose and fluid. By contrast, the packing within the inner leaflet at the same site would be compressed and more rigid. We suggest that this great difference in the packing of lipid molecules between the two lipid layers would be crucial for the merger of the outer leaflets, and then the inner leaflets, of the two membranes. In addition, the microprotrusion would require a rather small area of contact, minimizing the energy needed to overcome the repulsive forces between the apposing membranes (Rand, 1981).

Stegmann et al. (1990) proposed that the time lag before fusion is due to the aggregation of HA spikes in the contact zone of the virus–target membrane complex, and proposed a model fusion intermediate in which the fusion site was surrounded by multiple HA spikes. Similar models have also been proposed by others (Bentz et al., 1990; Bentz et al., 1993; Guy et al., 1992; Wilschut and Bron, 1993). Certain structural features seem common to the schematic drawings made by these authors and the microprotrusion we observed here (Fig. 12 *c*). First, HA induces bending of the apposing membranes, creating protuberances roughly as large as HA spikes. Second, because of this, the site of membrane contact is a local point only a few nanometers in diameter. Third, fusion may be initiated without the need for inverted micelles (except in the model proposed by Bentz et al., 1990).

However, with respect to the localization and morphology of spikes and IMPs, our observations are different from the previous models. Although all of the schematic drawings for the previous models include a fusion site closely surrounded by several HA spikes, we observed neither spikes nor IMPs just around the protrusions and the pits. Instead, we found that the large IMPs were ensconced in the centers of the pits. We suggest that the observed IMP might contain a portion of HA which penetrates into the liposomal membrane, since the IMPs were observed on the array of HA spikes on the viral surface, and also because isolated HA rosettes were observed as similar large IMPs on the concave face of the liposome under acidic conditions. In this case, the size of the IMPs, ~10 nm, seems to be rather large for only three fusion peptides. The IMP might thus consist of fusion peptides along with some other elements of HA and lipid molecules.

In addition, the schematic models proposed by Stegmann et al. (1990), Guy et al. (1992), and Wilschut and Bron (1993) appear to postulate bending or tilting of the spikes. However we found no evidence of microprotrusions associated with bent or tilted spikes. Also, when we examined the structure of viruses on mica under fusion-competent conditions, it was difficult for us to detect any drastic change in the overall morphology of the spikes. Based on these observations, we surmise that part of the HA spike may penetrate into the target membrane while the body of the spike is standing upright.

Therefore, it is possible to hypothesize another model for the fusion intermediate (Fig. 12 *d*). The standing HA spikes would tug and deform apposing membranes into the shape of a microprotrusion if the spikes were centrally located and deeply anchored to both of the membranes as IMPs. Because we observed that fusion necks bore no IMPs, we suggest that the IMP needs to move out from the microprotrusion by some unknown mechanism, since the initial fusion pore is formed between the two membranes.

Recently, Carr and Kim (1993) reported that a synthetic peptide corresponding to a "loop" region of the HA2 subunit form a coiled-coil upon acidification. They proposed a "spring-loaded" mechanism, in which the conversion of the loop to the coil extends the coiled-coil of the long α-helix and drives the fusion peptides 100 Å toward the top of the spike, thus allowing the peptides to insert themselves into the target membrane. Bullough et al. (1994) demonstrated the extended three-stranded coiled-coil in x-ray crystallographs of soluble trimeric fragments prepared from the acidic form of bromelain-released HA, thus confirming the model. They also reported a second major change in the bottom region of HA; the lowest part of the long α-helix became reversed upside down, which was thought to shorten the bottom region. Furthermore, Yu et al. (1994) used spin-labeled synthetic peptides to demonstrate that a certain part of the long helix next to the fusion peptide may be inserted into the apposed membrane. All these data seem to suggest that a considerable portion of the HA spike with the fusion peptides may be inserted into the target, while the body of the spike is kept upright (for reviews see Carr and Kim, 1994; Hughson, 1995).

Our observation that the microprotrusion does not accompany bent spikes but bears a large IMP ensconced in the center seems consistent with the spring-loaded mechanism. However, since we still know little about the structure of HA in the protein–lipid complex at the fusion site,

further studies are needed to clarify the relationship between the model schemes involving a spring-loaded mechanism, a fusion site surrounded by HA spikes, and a microprotrusion of the lipid bilayer with an IMP at its center.

In conclusion, we propose that the microprotrusion of the lipid bilayer is a structure that represents a fusion intermediate. We believe that protein-mediated fusion events must originate at the points where IMPs can be observed.

We gratefully acknowledge the technical assistance of Seiko Muto. We thank Hiroshi Miyamoto for useful discussions.

Received for publication 27 February 1997 and in revised form 7 March 1997.

References

Air, G.M., and W.G. Laver. 1986. The molecular basis of antigenic variation in influenza virus. *Adv. Virus Res.* 31:53–102.

Bartlett, G.R. 1959. Phosphorus assay in column chromatography. *J. Biol. Chem.* 234:466–468.

Bentz, J., H. Ellens, and D. Alford. 1990. An architecture for the fusion site of influenza hemagglutinin. *FEBS (Fed. Eur. Biochem. Soc.) Lett.* 276:1–5.

Bentz, J., H. Ellens, and D. Alford. 1993. Architecture of the influenza hemagglutinin fusion site. *In* Viral Fusion Mechanisms. J. Bentz, editor. CRC Press, Boca Raton, FL. 163–199.

Booy, F.P. 1993. Cryoelectron microscopy. *In* Viral Fusion Mechanisms. J. Bentz, editor. CRC Press, Boca Raton, FL. 21–54.

Brunner, J. 1989. Testing topological models for the membrane penetration of the fusion peptide of influenza virus hemagglutinin. *FEBS (Fed. Eur. Biochem. Soc.) Lett.* 257:369–372.

Brunner, J., and M. Tsurudome. 1993. Fusion-protein membrane interactions as studied by hydrophobic photolabeling. *In* Viral Fusion Mechanisms. J. Bentz, editor. CRC Press, Boca Raton, FL. 67–88.

Bullough, P.A., F.M. Hughson, J.J. Skehel, and D.C. Wiley. 1994. Structure of influenza haemagglutinin at the pH of membrane fusion. *Nature (Lond.).* 371:37–43.

Burger, K.N.J., G. Knoll, and A.J. Verkleij. 1988. Influenza virus-model membrane interaction. A morphological approach using modern cryotechniques. *Biochim. Biophys. Acta.* 939:89–101.

Carr, C.M., and P.S. Kim. 1993. A spring-loaded mechanism for the conformational change of influenza hemagglutinin. *Cell.* 73:823–832.

Carr, C.M., and P.S. Kim. 1994. Flu virus invasion: halfway there. *Science (Wash. DC).* 266:234–236.

Clague, M.J., C. Schoch, and R. Blumenthal. 1993. Toward a dissection of the influenza hemagglutinin-mediated membrane fusion pathway. *In* Viral Fusion Mechanisms. J. Bentz, editor. CRC Press, Boca Raton, FL. 113–132.

Cullis, P.R., and B. De Kruijff. 1979. Lipid polymorphism and the functional roles of lipids in biological membranes. *Biochim. Biophys. Acta.* 559:399–420.

Gething, M.J., J.M. White, and M.D. Waterfield. 1978. Purification of the fusion protein of Sendai virus: analysis of NH_2-terminal sequence generated during precursor activation. *Proc. Natl. Acad. Sci. USA.* 75:2737–2740.

Gething, M.-J., R.W. Doms, D. York, and J. White. 1986. Studies on the mechanism of membrane fusion: site-specific mutagenesis of the hemagglutinin of influenza virus. *J. Cell Biol.* 102:11–23.

Guy, H.R., S.R. Durell, C. Schoch, and R. Blumenthal. 1992. Analyzing the fusion process of influenza hemagglutinin by mutagenesis and molecular modeling. *Biophys. J.* 62:95–97.

Harter, C., P. James, T. Bächi, G. Semenza, and J. Brunner. 1989. Hydrophobic binding of the ectodomain of influenza hemagglutinin to membranes occurs through the "fusion peptide." *J. Biol. Chem.* 264:6459–6464.

Heuser, J. 1981. Preparing biological samples for stereo-microscopy by the quick-freeze, deep-etch, rotary-replication technique. *Methods Cell Biol.* 22: 97–122.

Heuser, J.E. 1983. Procedure for freeze-drying molecules adsorbed to mica flakes. *J. Mol. Biol.* 169:155–195.

Hughson, F.M. 1995. Structural characterization of viral fusion proteins. *Curr. Biol.* 5:265–274.

Kawasaki, K., S.B. Sato, and S. Ohnishi. 1983. Membrane fusion activity of reconstituted vesicles of influenza virus hemagglutinin glycoproteins. *Biochim. Biophys. Acta.* 733:286–290.

Kawasaki, K., and S. Ohnishi. 1992. Membrane fusion of influenza virus with phosphatidylcholine liposomes containing viral receptors. *Biochem. Biophys. Res. Commun.* 186:378–384.

Klenk, H.-D., R. Rott, M. Orlich, and J. Blodorn. 1975. Activation of influenza A viruses by trypsin treatment. *Virology.* 68:426–439.

Knoll, G., K.N.J. Burger, R. Bron, G. van Meer, and A.J. Verkleij. 1988. Fusion of liposomes with the plasma membrane of epithelial cells: fate of incorporated lipids as followed by freeze fracture and autoradiography of plastic sections. *J. Cell Biol.* 107:2511–2521.

Lazarowitz, S., and P.W. Choppin. 1975. Enhancement of the infectivity of influenza A and B viruses by proteolytic cleavage of the hemagglutinin polypeptide. *Virology.* 68:440–454.

Lowry, O.H., N.J. Rosebrough, A.L. Farr, and R.J. Randall. 1951. Protein measurement with the Folin phenol reagent. *J. Biol. Chem.* 193:265–275.

Ludwig, K., T. Korte, and A. Herrmann. 1995. Analysis of delay times of hemagglutinin-mediated fusion between influenza virus and cell membranes. *Eur. Biophys. J.* 24:55–64.

MacDonald, R.I., and R.C. MacDonald. 1975. Assembly of phospholipid vesicles bearing sialoglycoprotein from erythrocyte membrane. *J. Biol. Chem.* 250:9206–9214.

Maeda, T., A. Asano, K. Ohki, Y. Okada, and S. Ohnishi. 1975. A spin-label study on fusion of red blood cells induced by hemagglutinating virus of Japan. *Biochemistry.* 14:3736–3741.

Maeda, T., K. Kawasaki, and S. Ohnishi. 1981. Interaction of influenza virus hemagglutinin with target membrane lipids is a key step in virus-induced hemolysis and fusion at pH 5.2. *Proc. Natl. Acad. Sci. USA.* 78:4133–4137.

Matlin, K.S., H. Reggio, A. Helenius, and K. Simons. 1981. Infectious entry pathway of influenza virus in a canine kidney cell line. *J. Cell Biol.* 91:601–613.

Monck, J.R., and J.M. Fernandez. 1992. The exocytotic fusion pore. *J. Cell Biol.* 119:1395–1404.

Morris, S.J., D.P. Sarkar, J.M. White, and R. Blumenthal. 1989. Kinetics of pH-dependent fusion between 3T3 fibroblasts expressing influenza hemagglutinin and red blood cells. *J. Biol. Chem.* 264:3972–3978.

Ohnishi, S. 1988. Fusion of viral envelopes with cellular membranes. *In* Current Topics in Membranes and Transport. Vol. 32. N. Düzgünes and F. Bronner, editors. Academic Press, Orlando, FL. 257–296.

Rand, R.P. 1981. Interacting phospholipid bilayers: measured forces and induced structural changes. *Annu. Rev. Biophys. Bioeng.* 10:277–314.

Ruigrok, R.W.H., N.G. Wrigley, L.J. Calder, S. Cusack, S.A. Wharton, E.B. Brown, and J.J. Skehel. 1986. Electron microscopy of the low pH structure of influenza virus haemagglutinin. *EMBO (Eur. Mol. Biol. Organ.) J.* 5:41–49.

Sarkar, D.P., S.J. Morris, O. Eidelman, J. Zimmerberg, and R. Blumenthal. 1989. Initial stages of influenza hemagglutinin-induced cell fusion monitored simultaneously by two fluorescent events: cytoplasmic continuity and lipid mixing. *J. Cell Biol.* 109:113–122.

Segrest, J.P., T.M. Wilkinson, and L. Sheng. 1979. Isolation of glycophorin with deoxycholate. *Biochim. Biophys. Acta.* 554:533–537.

Singleton, W.S., M.S. Gray, M.L. Brown, and J.L. White. 1965. Chromatographically homogeneous lecithin from egg phospholipids. *J. Am. Oil Chem. Soc.* 42:53–56.

Skehel, J.J., A.J. Hay, and M.D. Waterfield. 1980. Influenza virus. *In* Cell Membranes and Viral Envelopes. Vol. 2. H.A. Blough and J.M. Tiffany, editors. Academic Press, Orlando, FL. 647–681.

Spruce, A.E., A. Iwata, J.M. White, and W. Almers. 1989. Patch clamp studies of single cell-fusion events mediated by a viral fusion protein. *Nature (Lond.).* 342:555–558.

Stegmann, T., R.W. Doms, and A. Helenius. 1989. Protein-mediated membrane fusion. *Annu. Rev. Biophys. Biophys. Chem.* 18:187–211.

Stegmann, T., and A. Helenius. 1993. Influenza virus fusion: from models toward a mechanism. *In* Viral Fusion Mechanisms. J. Bentz, editor. CRC Press, Boca Raton, FL. 89–111.

Stegmann, T., D. Hoekstra, G. Scherphof, and J. Wilschut. 1985. Kinetics of pH-dependent fusion between influenza virus and liposomes. *Biochemistry.* 24: 3107–3113.

Stegmann, T., D. Hoekstra, G. Scherphof, and J. Wilschut. 1986. Fusion activity of influenza virus: a comparison between biological and artificial target membrane vesicles. *J. Biol. Chem.* 261:10966–10969.

Stegmann, T., J.M. White, and A. Helenius. 1990. Intermediates in influenza induced membrane fusion. *EMBO (Eur. Mol. Biol. Organ.) J.* 9:4231–4241.

Verkleij, A.J. 1984. Lipidic intramembranous particles. *Biochim. Biophys. Acta.* 779:43–63.

White, J.M. 1990. Viral and cellular membrane fusion proteins. *Annu. Rev. Physiol.* 52:675–697.

White, J.M. 1992. Membrane fusion. *Science (Wash. DC).* 258:917–924.

White, J., J. Kartenbeck, and A. Helenius. 1982. Membrane fusion activity of influenza virus. *EMBO (Eur. Mol. Biol. Organ.) J.* 1:217–222.

White, J.M., and I.A. Wilson. 1987. Anti-peptide antibodies detect steps in a protein conformational change: low-pH activation of the influenza virus hemagglutinin. *J. Cell Biol.* 105:2887–2896.

Wiley, D.C., and J.J. Skehel. 1987. The structure and function of the hemagglutinin membrane glycoprotein of influenza virus. *Annu. Rev. Biochem.* 56:365–394.

Wilschut, J., and R. Bron. 1993. The influenza virus hemagglutinin: membrane fusion activity in intact virions and reconstituted virosomes. *In* Viral Fusion Mechanisms. J. Bentz, editor. CRC Press, Boca Raton, FL. 133–161.

Wilson, I.A., J.J. Skehel, and D.C. Wiley. 1981. Structure of the haemagglutinin membrane glycoprotein of influenza virus at 3 Å resolution. *Nature (Lond.).* 289:366–373.

Yoshimura, A., S. Yamashina, and S. Ohnishi. 1985. Mobilization and aggregation of integral membrane proteins in erythrocytes induced by interaction with influenza virus at acidic pH. *Exp. Cell Res.* 160:126–137.

Yu, Y.G., D.S. King, and Y-K. Shin. 1994. Insertion of a coiled-coil peptide from influenza virus hemagglutinin into membranes. *Science (Wash. DC).* 266:274–276.